# The Star Formation Reference Survey

A. Zezas[1,2,3] , on behalf of the Star Formation Reference Survey (SFRS) Team:

M. Ashby[3], P. Barmby[4], P. Bonfini[1,2], C. Cao[5], C. G. Fazio[3], E. Gonzalez-Alfonso[6], H. Kaneda[7], S. Madden[8], S. Mahajan[3,9], C. Papovich[10], S. Raychaudhury[9], H. A. Smith[3], E. Sturm[11], J. Surace[12], S. P. Willner[3], H. Wu[13], Y-N. Zhu[13]

(1) University of Crete (Greece), (2) FORTH (Greece), (3) Harvard-Smithsonian Center for Astrophysics (USA), (4) Univ. of Western Ontario (Canada), (5) Shandong Univ. at Weihai (China), (6) Universidad de Alcala (Spain), (7) Nagoya Univ. (Japan), (8) CEA/Saclay (France), (9) Univ. of Birmingham (U.K.), (10) Texas A&M University (USA), (11) MPE (Germany), (12) IPAC/Caltech (USA), (13) Chinese Academy of Sciences (China)

## Sample Selection

The sample used in the Star Formation Reference Survey (SFRS) is selected to span the full range of properties exhibited by star-forming galaxies in the local Universe. It is based on the PSCz catalog of IRAS detected star-forming galaxies (Saunders etal 2000). The sample covers the three-dimensional space defined by the full ranges spanned by PSCz galaxies in 60 μm luminosity (F60; a star-formation rate proxy), flux ratio F60/Ks (a specific star-formation rate proxy), and far-infrared color (F60/F100, Figure 1). This 3-D parameter space was binned and a representative set of galaxies in each 3D bin was selected. This process resulted in 369 galaxies *which cover the entire range of star formation properties seen locally: five decades in luminosity (and thus SFR); a factor of nearly 200 in specific SFR, and all masses, morphologies, and sizes.*

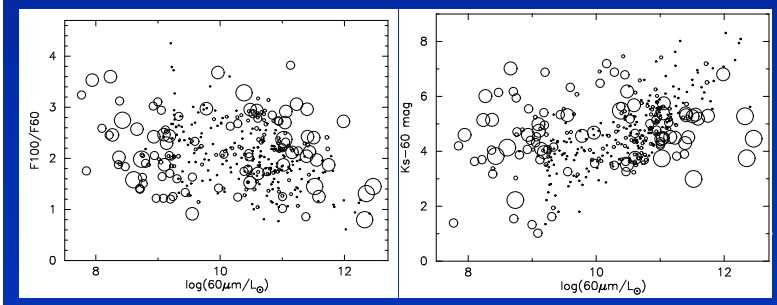


**Fig.1**: Projections of the 3D SFRS galaxy distribution into the 2-D spaces defined by 60 μm luminosity and far-infrared flux ratio **(Left)**, and the 60 μm luminosity and near- to far-infrared color (specific SFR proxy; **Right**). Large symbols indicate relatively rare objects that occupy sparsely-populated bins, providing a wider coverage of the galaxy parameter space (Ashby etal, in prep).

## Multiwavelength data

Key for any unbiased study of star-forming activity in galaxies, is the use of multiwavelength star-formation indicators. For this reason we have embarked in an ambitious multi-wavelength campaign to obtain complete coverage of the SFRS galaxies from radio to X-ray wavelengths (e.g. Fig 2). The status of this campaign is presented in Table 1. These data will provide, in addition to various star-formation rate indicators, quantitative measurements of the galaxies' morphology and stellar mass, diagnostics for AGN activity, and measurements of the metallicity in nuclear star-forming regions.

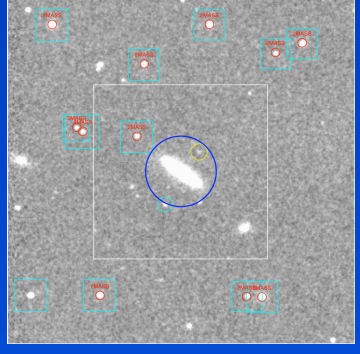

**Fig.2**: Example of the pipeline analysis of PAIRITEL NIR data to measure the morphology and total brightness of SFRS galaxies. The pipeline identifies the target (circled in blue) and any blended extended and point-like objects (which are fitted together with the target; shown in yellow and cyan respectively. The cyan squares indicate stars which are used for the photometric calibration of the PAIRITEL data (based on their 2MASS magnitudes; Bonfini etal, in prep).

## Goals

By having both a statistical sample of galaxies and a complete sampling of the SEDs from the X-ray/UV to the far-IR and radio,allows us to:

**a)** cross-calibrate the majority of star-formation rate indicators in different types of galaxies (e.g. Fig 3).
**b)** determine the relationships between star-formation rate (SFR) and fundamental galaxy parameters.
**c)** obtain a definitive census of star formation rate density in the local Universe.

In addition we will be able to create template galaxy SEDs representative of different types of galaxies, and understand how star-formation rates measured using different proxies depend on global galaxy properties.

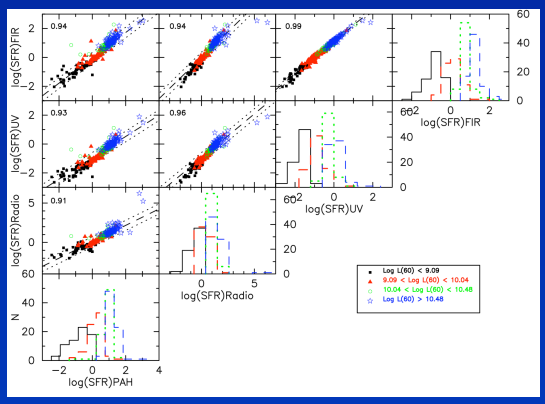


**Fig.3**: Correlations and distributions between SFRs estimated from different proxies for the 294 SFRS galaxies for which GALEX data are available in data release 4/5. In each panel the best fit correlation is shown by the solid line and its mean absolute deviation by the dashed line. The correlation coefficient for each set is shown in the upper left corner of each panel (Mahayan etal, in prep).

| Waveband | Observatory | Coverage |
|---|---|---|
| 1.4GHz | VLA/NVSS | 100% |
| 12,25,60,100 μm | IRAS | 100% |
| 65,90,140,160 μm | AKARI FIR All-Sky Survey | 95% |
| 12, 23 μm | WISE | 100% * |
| 24 μm | Spitzer/MIPS | 70% |
| 3.6, 4.5, 5.8, 8.0 μm | Spitzer/IRAC | 100% |
| JHKs | 2MASS | 100% |
| JHKs | PAIRITEL | 70% * |
| Y | Pan-STARRS | 100% * |
| ugriz | SDSS | 100% |
| Optical Spectra | SDSS (fiber) | 210/369 |
| Optical Spectra | FAST (longslit) | 100/369 * |
| Hα | NAOC | 30% * |
| 0.13–0.28 μm | GALEX | 90% to date |
| 0.5-8.0 keV (X-ray) | Chandra, XMM | > 50% |

**Table 1**: Multiwavelength coverage of the SFRS (* on-going survey or observing campaign)